Analytical solution of collisional sheet flows

Diego Berzi[1]

[1] Assistant professor, Dept. of Environmental, Hydraulic, Infrastructure, and Surveying Engineering, Politecnico di Milano, Milan, 20133, Italy. Email: diego.berzi@polimi.it

Abstract

This work focuses on the sediment transport that is dominated by collisional exchange of momentum between the particles and can be identified as the transition regime between bed and suspended load. Idealizing the particles as inelastic, frictional spheres and accounting for the role of the interstitial fluid on particle collisions, three regions characterize such flows: one diffuse collisional layer neighboring the free surface where a simple trapezium rule is employed to solve a boundary-value problem based on the kinetic theory; one dense, algebraic layer, in which there is an algebraic balance between production and dissipation of particle fluctuation energy, the concentration is approximately constant and correlated motion between the particles exists; one macro-viscous-layer, close to the erodible bed, where the collisions are inelastic and the fluid viscous force dominates the momentum exchange. Using boundary conditions of no-slip and yielding at the erodible bed and vanishing of the particle stresses and energy flux at the top of the sediments, an analytical description of the flow field is obtained. After a sensitivity analysis of the approximate theoretical solution to the model parameters - only one of them has though a phenomenological origin and cannot be directly measured - comparisons with experiments performed on sheet flows of water and plastic cylinders, sand or gravel assess the validity of the theory.

Introduction

The sheet flow is a particular regime of sediment transport where massive flow of sediments takes place near a bed and the particles are supported by their collisions and the turbulent fluctuations of the fluid velocity (Jenkins and Hanes 1998, and references therein). When the former mechanism is dominant, sheet flows are called collisional. The collisional sheet flow can be considered as an intermediate regime between bed-load and suspended-load. As pointed out by Jenkins and Hanes (1998), collisional sheet flows are rather extreme events, given the high fluid shear velocity necessary for them to develop; nonetheless, beside the interest for coastal and civil engineering (a large amount of sediments is indeed associated with unidirectional and oscillatory marine turbulent flows and sandstorms), they share some characteristics with the so called over-saturated debris flows (Armanini et al. 2005; Fraccarollo and Rosatti 2009; Berzi et al. 2010), i.e., debris flows where the top of the fluid is higher than the top of the particles. Modeling collisional sheet flows on the basis of a micro-mechanical description of particle interactions is therefore a first step towards a more fundamental approach to debris flows.

Here, the collisional sheet flow is idealized as a steady and fully developed horizontal flow of identical, inelastic, frictional spheres, driven into collisions by the shear stress exerted by the fluid at the top of them. Kinetic theories (Jenkins and Savage 1983; Savage 1984; Garzo and Dufty 1999) are employed to model the particle momentum exchange in the upper part of the flow. In doing so, the presence of a ballistic layer (Pasini and Jenkins 2005), in which the mean inter-particle distance is greater than the mean free path between particle encounters, is ignored; this is certainly not possible in the case of bed-load (Bagnold 1973). At the macroscopic scale, the interstitial fluid transmits only buoyancy and drag to the particles, while, at the microscopic scale, it affects also the inter-particle collisions. The latter phenomenon is captured through the dependence of the restitution coefficient, ratio of post to

pre-collisional relative velocity between two colliding particles, on the Stokes number (Joseph et al. 2001). This is an important difference between the present work and that of Jenkins and Hanes (1998). The dependence of the restitution coefficient on the Stokes number has been shown also in experiments on uniform debris flows (Armanini et al. 2005). It implies that, at a certain distance from the bed, here defined using a yield criterion, as in Berzi and Jenkins (2008a,b, 2009, 2011) and Jenkins and Berzi (2010), the collisions become perfectly inelastic. There, the momentum exchange is dominated by the fluid viscous force, and the associated flow regime is called macro-viscous (Bagnold 1954).

Similarly to what Berzi and Jenkins (2011) have done for the flows of inelastic spheres at the surface of an erodible bed in absence of interstitial fluid, three different layers are identified and treated separately. Near the free surface, there is a diffuse region, in which the particle interactions are essentially chaotic, binary, instantaneous collisions (Goldhirsch 2003), and the diffusion of particle fluctuation energy must be taken into account; the use of the trapezium rule of integration allows here to solve, in an approximate way, the differential equations of kinetic theory. Moving from this region into the interior, there is a transition to a dense collisional regime, where correlated motion plays a fundamental role (Jenkins 2006, 2007); assuming that an algebraic balance between production and dissipation of particle fluctuation energy holds and that the concentration is approximately constant, the derivation of an analytical solution to the flow in this dense algebraic layer is possible. Finally, In the macro-viscous layer near the bed, where a shear rigidity develops (Goldman and Swinney 2006), the mixture is treated as a viscous dense suspension, with the concentration-dependence of the viscosity suggested by the experiments of Ovarlez et al. (2006).

The aforementioned procedure allows to obtain a complete analytical solution to the collisional sheet flow. Firstly, the dependence of the analytical solution on the parameters of the model is analyzed. All of them but one are though physically based parameters, so that

they can be measured. Then, the prediction of the present theory are compared with the results of experiments on the flow of different types of granular material (plastic cylinders, sand and gravel) and water.

Governing equations

A sketch of the flow configuration is given in Fig.1, together with the concentration profile assumed in the present work. Here, ρ denote the fluid mass density, ν the particle concentration, g the gravitational acceleration, σ the particle specific mass, d the particle diameter, η the fluid viscosity, U the fluid velocity, and u the particle velocity. The Reynolds number $\mathrm{R} \equiv \rho d\left[g\left(\sigma-1\right) d / \sigma \right]^{1/2} / \eta$ characterizes the fall velocity of the particles. In what follows, all quantities are made dimensionless using the particle diameter, the mass density of the particle material, $\rho\sigma$, and the reduced gravity, $g\left(\sigma-1\right)/\sigma$. The flow is assumed to be steady and fully developed in the horizontal x-direction; the y coordinate is taken to be perpendicular to the free surface, with $y = 0$ at the bed and $y = h$ at the free surface. There is a diffuse collisional layer at the top, located in the region $H \le y \le h$, a core region (the dense algebraic layer) of extent $H-\delta$, in which there is an algebraic balance between production and dissipation of collisional fluctuation energy, and a macro-viscous layer, for $0 \le y \le \delta$, where the fluid viscosity dominates the momentum exchange. The dimensionless shear stress exerted by the fluid at the top of the diffuse collisional layer that drives the particles into collisions is the Shields parameter, θ. In what follows, all terms involving spatial variation along the spanwise direction, as well as the additional force due to the lateral confinement to the flow (Jop et al. 2005), are neglected; this is possible if the ratio of particle depth to channel width is much less than one (Berzi et al. 2010), as is the case of the experiments reported in the next section.

The collisional interactions are supposed strong enough to suspend the particles without being affected by the fluid turbulent velocity fluctuations. A criterion for the latter requirement is that the ratio of the particle settling velocity, w, to the fluid turbulent shear velocity, $(\theta\sigma)^{1/2}$, at $y = h$ must be greater than one, as suggested by Jenkins and Hanes (1998); on the other hand, Chanson (1999) reported that, for the inception of massive transport, $w/(\theta\sigma)^{1/2}$ must be less than 0.5 to 5. Hence, at a first approximation, the present theoretical treatment holds for $1 \leq w/(\theta\sigma)^{1/2} \leq 5$.

The balances of particle momentum parallel and perpendicular to the flow are

$$s' = -D, \tag{1}$$

and

$$p' = -\nu, \tag{2}$$

respectively, where s is the particle shear stress, p the particle pressure and D the drag force exerted on the particles by the fluid. Here, and in what follows, a prime indicates a spatial derivative along y.

The balance of fluid momentum parallel to the flow is simply

$$S' = D, \tag{3}$$

where S is the fluid shear stress. Here, the horizontal fluid pressure gradient is ignored by assuming that the depth of the clear fluid above is much greater than h (boundary layer approximation).

The balance of particle fluctuation energy in the collisional layers ($\delta \leq y \leq h$) is

$$Q' = su' - \Gamma, \tag{4}$$

where Q is the particle energy flux in the y-direction, and Γ is the rate of collisional dissipation. When the diffusive term on the left hand side of Eq. (4) is negligible, the

production of fluctuation energy due to the working of the stress equals the dissipation due to collisions; Jenkins and Berzi (2010) refer to this as the algebraic balance.

To close the problem, I use, in the diffuse collisional and dense algebraic layers, the constitutive relations (Tab. 1), from the kinetic theory of Garzo and Dufty (1999), for frictionless, inelastic spheres, with the modifications suggested by Jenkins and Berzi (2010) to include the role of friction and the correlated motion between the particles. There, T is the granular temperature (one-third the mean square of the particle velocity fluctuations), n is the coefficient of normal restitution, and β is the coefficient of tangential restitution in a sticking collision. As in Jenkins and Berzi (2010), ε is an effective coefficient of restitution that incorporates the effects of friction in the limit of infinite friction (Herbst et al. 2000), when no fluid is present. In Tab. 1, G is the product of ν and the radial distribution function at contact. Although different expressions for the latter are available (Torquato 1995; Jenkins and Berzi 2010), they all tend to unity as the concentration tends to zero and to infinity as the concentration tends to the random close packing; I refer to these conditions as the dilute and the dense limit, respectively. The relation proposed by Barnocki and Davis (1988), as reported in Joseph et al. (2001), for the dependence of the restitution coefficient, e, on the Stokes number, $\mathrm{St} \equiv \sigma T^{1/2} \mathrm{R}/9$, is used to capture the influence of the fluid on the micromechanics of the particle collisions:

$$e \equiv \varepsilon - 6.9 \frac{1+\varepsilon}{\mathrm{St}}. \tag{5}$$

In the definition of the Stokes number, the square root of the granular temperature is a measure of the relative velocity between two colliding particles (as in Armanini et al 2005). The correlation length L that appears in the constitutive expression of the rate of collisional dissipation Jenkins (2006, 2007) accounts for the correlated motion between particles that is

likely to occur when the flow is dense. In the constitutive expression of L reported in Table 1, c is a constant of order unity.

Eq. (5) implies that the smaller the Stokes number, the more inelastic are the particle collisions. For $\mathrm{St} \le 6.9(1+\varepsilon)/\varepsilon$, the collisions are perfectly inelastic; hence, the fluid viscous forces dominate the momentum exchange and the flow regime becomes macro-viscous (Bagnold 1954). Given the definition of the Stokes number, its smallest values characterize the region near the bed, where the granular temperature approaches zero; there, as already mentioned, a macro-viscous layer develops, with the particles having approximately the same velocity of the fluid. The mixture reduces therefore to a single-phase fluid (dense suspension) whose shear stress obeys a viscous law with a viscosity coefficient depending on the particle concentration (see next section).

Approximate analytical solution

As already mentioned, to obtain an approximate analytical solution to the flow of Fig. 1, the three layers are treated separately. For the diffuse collisional layer, as in Berzi and Jenkins (2011), the trapezium rule - $\int_a^b \psi \mathrm{d}y \approx (b-a)(\psi_a+\psi_b)/2$, where, from this point onward, the subscript indicates the position y at which the generic variable ψ is evaluated – allows to obtain an analytical approximate integration of the balance Eqs. (1)-(4) and the constitutive relations for the shear stress of Tab. 1. The concentration is taken to be approximately constant, and equal to $\bar{\nu}$, in the dense algebraic and macro-viscous layers, and approximately linearly distributed between zero and $\bar{\nu}$ in the diffuse layer (see Fig. 1); the experimental observations of Pugh and Wilson (1999) support the validity of this assumption.

Diffuse collisional layer ($H \le y \le h$)

The particle stresses and energy flux approximately vanish at the free surface. From Eqs. (1)-(3), and using the boundary conditions $p_h = s_h = 0$ and $S_h = \theta$,

$$s + S = \theta . \tag{6}$$

This relation holds everywhere in the flow and not only in the diffuse collisional layer.

Following Berzi and Jenkins (2011), the concentration at the free surface is very small and the algebraic layer is entirely dense, with $L = 1$ at $y = H$. Neglecting the divergence of Q and using the constitutive relation for L in the dense algebraic layer, the energy balance (4) reduces to an algebraic relation between granular temperature and shear rate:

$$\left(\frac{u'}{T^{1/2}} \right)^3 = \frac{15}{J} \frac{(1-e^2)}{cG^{1/3}} . \tag{7}$$

L and s/p can now be expressed as functions of ν and e (see Jenkins and Berzi 2010 for more details) as

$$L = \frac{1}{2} \left[\frac{15}{J} \left(1-e^2\right) c^2 \right]^{1/3} G^{2/9} \tag{8}$$

and

$$\frac{s}{p} = \left[\frac{192}{25\pi^{3/2}} \frac{J^2 \left(1-e\right)}{c\left(1+e\right)^2} \right]^{1/3} \frac{1}{G^{1/9}} . \tag{9}$$

Employing Eq. (8) in Eq. (9), with the condition $L_H = 1$, I obtain the value, k, of the stress ratio s/p at $y = H$:

$$k = \left(\frac{24 J_H}{5\pi} \frac{1-e_H}{1+e_H} \right)^{1/2} , \tag{10}$$

where, upon taking the dense limit (i.e., $G \to \infty$) in the expression for J of Tab. 1, $J_H = \left(1+e_H\right)/2 + \left(\pi/4\right)\left(3e_H - 1\right)\left(1+e_H\right)^2 / \left[24 - \left(1-e_H\right)\left(11-e_H\right)\right]$. The value of k is, therefore, solely determined by the value of the coefficient of restitution at $y = H$.

The use of the trapezium rule in Eq. (2), with $p_h = 0$, $\nu_h = 0$, and taking ν_H to be $\bar{\nu}$, gives

$$p_H = \bar{\nu}\left(h - H\right)/2 . \tag{11}$$

Then, Eqs. (11) and (10) used in Eq. (6), and neglecting S with respect to s in the dense algebraic layer (Berzi et al. 2010), provides the value of the depth of the diffuse collisional layer:

$$h - H = \frac{2\theta}{\bar{\nu}k} . \tag{12}$$

The determination of $h - H$ is not straightforward, though, given that the value of e_H, necessary to evaluate k from Eq. (10), can be obtained from Eq. (5) only if the value of St_H is known; the latter though depends on the granular temperature at $y = H$,

$$T_H = \frac{p_H}{2\bar{\nu}G_H\left(1 + e_H\right)}, \tag{13}$$

which is also a function of e_H and, through p_H, $h - H$. In Eq. (13), G_H is obtained from Eq. (8) with $L = 1$. However, a simple iterative method provides the values of $h - H$, e_H and T_H.

The performed analysis holds as long as $e_H > 0$; if $e_H = 0$, only the diffuse collisional and macro-viscous layers are present in the flow. The value of the coefficient of restitution at $y = H$ is an increasing function of the depth of the diffuse collisional layer, and therefore an increasing function of θ. The minimum value of the Shields parameter, $\breve{\theta}$, for having a dense algebraic layer follows from Eqs. (10)-(13), using the condition $e_H = 0$,

$$\breve{\theta} = 1.64\left(\frac{4 - 2\pi/13}{15c^2}\right)^{3/2} \bar{\nu}\breve{T}, \tag{14}$$

where $\breve{T} = 81\left[6.9\left(1+\varepsilon\right)/\varepsilon\right]^2/\left(\sigma^2 \mathrm{R}^2\right)$ is the minimum temperature in the collisional layers associated with the value of the Stokes number at which the collisions are perfectly inelastic.

For $\theta \le \breve{\theta}$, Eq. (12) still provides the depth of the diffuse collisional layer, with $k \approx 0.82$, from Eq. (10) with $e_H = 0$.

The particle velocity at the top of the diffuse collisional layer follows from the constitutive relation for the particle shear stress of Tab. 1 and the trapezium rule,

$$u_h = u_H + \left(\frac{5\pi^{1/2} s_h F_h}{2 J_h \nu_h T_h^{1/2}} + \frac{5\pi^{1/2} F_H T_H^{1/2}}{2 J_H} k \right) \frac{(h-H)}{2}. \tag{15}$$

The first term between brackets on the right hand side of Eq. (15) is proportional to s_h, as it is easy to show by taking the dilute limit (i.e., $G \to \nu$) in the expressions of Table 1: $G_h = \nu_h$, $F_h = (4\nu_h)^{-1}$, and $J_h = 25\pi/32\left[24 - 6(1-e_h)^2 - 5(1-e_h^2)\right]^{-1} \nu_h^{-2}$. Hence, with $s_h = 0$,

$$u_h = u_H + \frac{5(1+e_H) k (\pi T_H)^{1/2}}{8 J_H} (h-H). \tag{16}$$

Finally, the volume flow rate per unit width of the particles, at $y = h$, is calculated as

$$q_h = q_H + \bar{\nu}(u_h + u_H)(h-H)/4. \tag{17}$$

The values of q_H and u_H are determined as part of the solution for the dense algebraic layer.

Dense algebraic layer ($\delta \le y \le H$)

Given that the flow is dense in both the dense algebraic and the macro-viscous layers, the pressure distribution there is given to a good approximation by

$$p = p_H + \bar{\nu}(H - y). \tag{18}$$

Then, the depth of the dense algebraic layer can be determined from Eq. (6), with $p = p_\delta$ evaluated with Eq. (18), as

$$H - \delta = \frac{\theta}{\bar{\nu}} \left(\frac{1}{s_\delta / p_\delta} - \frac{1}{k} \right). \tag{19}$$

For $\theta > \breve{\theta}$, the particle stress ratio at $y = \delta$ reads

$$\frac{s_\delta}{p_\delta}=\left[\frac{2\bar{\nu}\breve{T}}{\theta}\left(\frac{192}{25\pi^{3/2}}\frac{J_\delta^{\,2}}{c}\right)^3\right]^{1/8}, \tag{20}$$

from Eq. (6), with $p_\delta = 2\bar{\nu}G_\delta T_\delta$ and G_δ evaluated from Eq. (9), with $T_\delta = \breve{T}$ and $J_\delta = 1/2 - \pi/52$, given that $e_\delta = 0$. For $\theta \le \breve{\theta}$, instead, $s_\delta / p_\delta = k$ (the dense algebraic layer vanishes).

From the constitutive relations for the particle shear stress and pressure of Tab. 1,

$$u' = \left[\frac{25\pi(1+\bar{e})}{32\bar{\nu}\bar{G}\bar{J}^2}\right]^{1/2}\frac{s}{p}\,p^{1/2}, \tag{21}$$

where, as in Jenkins and Berzi (2010), $\bar{J}$ and $\bar{G}$ are the values of J and G calculated from Tab. 1 and Eq. (9), using $\bar{e} = (e_H + e_\delta)/2$ and $\overline{s/p} = (k + s_\delta / p_\delta)/2$, the average values of the coefficient of restitution and the particle stress ratio in the dense algebraic layer, respectively. Then, using Eqs. (2-2) and (3-1) in Eq. (3-16), and integrating, with the boundary condition $u = u_\delta$, when $p = p_\delta$, gives

$$u = u_\delta + 2A\theta\left(p_\delta^{\,1/2} - p^{1/2}\right), \tag{22}$$

where $A = \left[25\pi(1+\bar{e})\right]^{1/2} / \left[32\bar{\nu}^3\bar{G}\bar{J}^2\right]^{1/2}$. Eq. (22) provides the value u_H of Eqs. (16) and (17) when $p = p_H$.

The integration of the product of the concentration and the velocity profile given by Eq. (22) in the dense algebraic layer provides the value of the volume flow rate per unit width of the particles at $y = H$:

$$q_H = q_\delta + u_\delta\bar{\nu}(H-\delta) + \frac{2}{3}A\theta p_\delta^{\,3/2}\left[1 - 3\frac{p_H}{p_\delta} + 2\left(\frac{p_H}{p_\delta}\right)^{3/2}\right], \tag{23}$$

where q_δ and u_δ are evaluated from the solution of the macro-viscous layer.

Macro-viscous layer ($0 \le y \le \delta$)

The depth of the macro-viscous layer can be determined from Eq. (6), with $p = p_0$ evaluated with Eq. (18), as

$$\delta = \frac{\theta}{\bar{\nu}}\left(\frac{1}{\alpha} - \frac{1}{s_\delta / p_\delta}\right). \tag{24}$$

Here, α is the value of the stress ratio at the bed for which the particles develop a shear rigidity (Jenkins and Berzi 2010; Berzi et al. 2010; Berzi and Jenkins 2011) and represents a material parameter.

The macro-viscous layer, then, vanish when $s_\delta / p_\delta = \alpha$, i.e., from Eq. (20), when

$$\theta = \breve{\theta} = 2\bar{\nu}\breve{T}\left[192\left(1/2 - \pi/52\right)^2 / \left(25c\pi^{3/2}\right)\right]^3 / \alpha^8. \tag{25}$$

For $\theta > \breve{\theta}$, however, the analysis performed on the dense algebraic layer still holds; the non-zero value of the coefficient of restitution at the bed, $e_0 = e_\delta$, is though now required to evaluate the average coefficient of restitution in the dense algebraic layer, $\bar{e}$. The condition $\alpha = \theta / p_0$, from Eq. (6), with $p_0 = 2\bar{\nu}\left(1 + e_0\right)G_0 T_0$, where G_0 is given by Eq. (9) and T_0 by the definition of the Stokes number, provides an implicit equation that can be easily solved to determine e_0.

Eqs. (12), (19) and (24) give the total depth of the sheet flow,

$$h = \frac{\theta}{\bar{\nu}}\left(\frac{1}{\alpha} + \frac{1}{k}\right). \tag{26}$$

As already mentioned, in the macro-viscous layer, the total (particle plus fluid) shear stress obeys to a viscous law,

$$\theta = \frac{u'}{\sigma \mathrm{R}^*}, \tag{27}$$

where R^* is a modified Reynolds number that takes into account the effect of the particle concentration on the viscosity. Ovarlez et al. (2006) obtained a Krieger-Dougherty (1959)

expression for the concentration-dependence of the viscosity, with a divergence exponent equal to 2 and a singularity at around 0.6 for polystyrene beads. The latter coincides with the random close packing value adopted by Jenkins and Berzi (2010) where the radial distribution function, G/ν, is singular. Here, I therefore use

$$\mathrm{R}^{*} = \frac{\mathrm{R}}{\left(\tilde{G}/\bar{\nu}\right)^{2}}, \tag{28}$$

where $\tilde{G}$ is the average value of the function G in the macro-viscous layer, associated with the average particle stress ratio, $\left(s_{\delta}/p_{\delta}+\alpha\right)/2$. As in Cassar et al. (2005), the dependence of the concentration on the particle stress ratio is taken to be the same with or without the interstitial fluid, so that $\tilde{G}$ is evaluated from Eq. (9). This allows to apply the present theory without requiring to know the actual form of the radial distribution function, which is still an open question also for the highly idealized case of mono-dispersed, rigid spheres (e.g., Mitarai and Nakanishi 2007).

Integrating Eq. (27), with the boundary condition $u = 0$ when $y = 0$, gives the velocity profile in the macro-viscous layer,

$$u = \sigma \mathrm{R}^{*} \theta y. \tag{29}$$

Finally, the integration of the product of the concentration and the velocity profile of Eq. (29) between 0 and δ leads to the volume flow rate per unit width of the particles at $y = \delta$,

$$q_{\delta} = \frac{\bar{\nu}}{2} \sigma \mathrm{R}^{*} \theta \delta^{2}. \tag{30}$$

Results

The above described, approximate, analytical solution to collisional sheet flows requires the knowledge of the properties of the granular material and interstitial fluid: the restitution coefficient in dry conditions, ε; yield stress ratio, α; coefficient, c, of the correlation length; particle specific mass, σ; assumed constant concentration in the dense layers, $\bar{\nu}$; and Reynolds number, R. Then, the particle depth, h, and the volume flow rate per unit width of the particles, $q = q_h$, can be obtained as functions of the Shields parameter θ.

Firstly, I check the sensitivity of the present analytical solution to the material properties. Then, I make comparisons with the experiments performed by Smart (1984), Rickenmann (1991), Nnadi and Wilson (1992) and Sumer et al. (1996). In what follows, if not stated otherwise, the results refer to a range of the Shields parameter, θ, for which $1 \le w/(\sigma\theta)^{1/2} \le 5$, where $w = \sigma/\left[18/\mathrm{R} + (0.75\sigma)^{1/2}\right]$, valid for natural particles (Ferguson and Church 2004).

The material properties of 3 mm glass spheres and water, as suggested by Jenkins and Berzi (2010) and Berzi and Jenkins (2011), represents the reference set of parameters for the sensitivity analysis: $\varepsilon = 0.60$, $\alpha = 0.40$, $c = 0.50$, $\sigma = 2.6$, $\bar{\nu} = 0.60$ and $\mathrm{R} \approx 400$. With these, $w = 1.8$, $\breve{\theta} \approx 0.02$ (vanishing of the dense algebraic layer) and $\hat{\theta} \approx 6.90$ (vanishing of the macro-viscous layer). Hence, for the entire range of the Shields parameter for which the sediment transport can be defined as collisional sheet flow, $0.05 \le \theta \le 1.25$, the three layers of Fig. 1 are always present.

Fig. 2a shows that the particle flow rate, at a given Shields parameter, decreases if the restitution coefficient in dry condition increases from 0.60 to 0.90, i.e. from very to slightly inelastic particles. This apparently counter-intuitive result is due to the fact that, as already noticed by Jenkins and Hanes (1998), a higher coefficient of restitution gives a thicker flow, at a given θ; hence, the same force driving particles into collisions acts on a higher number of

particles, resulting in a slower flow and in a diminished flow rate. Increasing the yield stress ratio, that can be interpreted as the tangent of the angle of repose of the particles (Berzi and Jenkins 2011), does not affect the results, at least until a macro-viscous layer is present in the flow (Fig. 2b); this is due to the high viscosity of the dense suspension in the macro-viscous layer that implies small particle velocities, and therefore a negligible contribution, q_δ, on q. The parameter c in the correlation length introduced by Jenkins (2006, 2007) plays an important role (Fig. 2c); the particle flow rate is indeed roughly proportional to c. This parameter has a phenomenological origin (Jenkins 2006, 2007), so that it cannot be directly measured, but must be tuned on the basis of fitting with experiments. However, the influence of the parameter c is much less pronounced on the particle depth, as pointed out later. As shown by Eqs. (30), (23) and (17), the adopted non-dimensionalisation entirely captures the role of the particle specific mass in the collisional layers, but not in the macro-viscous layer; this explains the slight difference in the curves observed in Fig 2d. Fig. 2e shows that the value of the approximately constant concentration in the dense algebraic and macro-viscous layers plays a certain role in the evaluation of the particle flow rate. In absence of direct measurements of the concentration profile, Berzi et al. (2010) have suggested that it is possible to infer this concentration from the ratio of particle to total (particle plus fluid) flow rate per unit width, in the case of uniform, fully-saturated (i.e. height of the particles equal to the height of the fluid) debris flows over erodible beds. Finally, Fig. 2f highlights the role of the Reynolds number of the particles. The values $\mathrm{R} \approx 2500$ and $\mathrm{R} \approx 10$ correspond, for instance, to glass spheres of diameter equal to 10 and 0.3 mm, respectively, immersed in water. The curves roughly collapse at large Reynolds numbers, while for small R (i.e., small particle size or, equivalently, high fluid viscosity), the mobility of the particles decreases with R (q decreases at a given θ); the range of applicability of the present theory (the range of the Shields parameter corresponding to collisional sheet flows), however, increases with R.

The analytical solution is now compared with the experiments performed by Sumer et al. (1996) with mono-dispersed plastic cylinders and water in a horizontal, closed, rectangular channel of width 0.3 m; the ratio of particle depth to channel width is of order 0.1 in all the experiments performed by the authors, so that the role of the sidewalls can be ignored. Sumer and co-workers used two types of particles: circular cylinders 3 mm in height and 3 mm in diameter with $\sigma = 1.27$; and elliptic cylinders 3.3 mm in height and axes 1.9 mm and 2.8 mm with $\sigma = 1.14$. I therefore set $\varepsilon = 0.6$, obtained from the expression of Table 1, with $n = 0.93$ and $\beta = 0.22$, the values measured for 3 mm acrylic spheres by Lorenz et al. (1997); $\alpha = 0.50$, roughly equal to the tangent of 27°, which is the angle of repose of the plastic cylinders submerged in water measured by Sumer et al. (1996); $\sigma = 1.20$, $w = 1.40$ and $R = 190$, which are the average specific mass, settling velocity and Reynolds number, respectively, of the two types of plastic particles employed by Sumer et al. (1996); $\overline{\nu} = 0.55$, which is actually very close to the so called transport concentration (ratio of particle to total flow rate per unit width) measured by Armanini et al. (2005) in the case of uniform, fully-saturated debris flows over erodible beds of plastic cylinders and water; $c = 0.50$, as for the case of 3 mm glass spheres, given that the effective coefficient of restitution in dry condition is the same, and the correlated motion between the particles is a well-known consequence of the inelasticity (Olafsen and Urbach 1998). An indirect way of assessing the validity of this choice will be reported later. With those parameters, $\breve{\theta} \approx 0.43$ and $\hat{\theta} \approx 22.64$; given that the values of the Shields parameter investigated by Sumer et al. (1996) are greater than 0.6, the three layers of Fig. 1 are always present.

Fig. 3a shows the comparison between the present analytical solution and the experiments performed by Sumer et al. (1996) in terms of particle depth against the Shields parameter. The present theory predicts a linear increasing of h with θ, as in Wilson's (1987) theory, and the agreement with the experiments is notable; the particle depth is well predicted by the

present theory also when the inter-particle collisions are, at least in the upper part of the flow, affected by the fluid turbulent velocity fluctuations - at the highest values of θ, for which $w/(\sigma\theta)^{1/2}$ is as low as 0.80.

Fig. 3b shows the values of u_h, u_H, and u_δ, scaled using the shear velocity $(\sigma\theta)^{1/2}$, predicted by the present theory as a function of the distance y from the bed, for three values of the Shields parameter, θ = 1.60, 1.00 and 0.50. The same plot also depicts the fluid velocity profiles obtained from:

$$\frac{U}{(\sigma\theta)^{1/2}} = 2.5\,\theta^{-3/4} y^{3/4}, \tag{31}$$

as derived by Sumer et al. (1996) on the basis of their experiments. As expected, when θ is small, i.e., $w/(\sigma\theta)^{1/2}$ is great, the particle inertia is greater than the fluid turbulence and the particles do not 'follow' the fluid (the particle and fluid velocities are significantly different). On the other hand, when θ = 1.60, i.e., $w/(\sigma\theta)^{1/2} \approx 1$, the particle and fluid velocities are similar. This is an indirect confirmation that the value $c = 0.50$ allows for the theoretical solution to reproduce the experiments.

Fig. 4 shows the comparisons between the results of the present theory and the experiments performed by Smart (1984), Rickenmann (1991) and Nnadi and Wilson (1992), using sand or gravel in water, as selected by Abrahams (2003) to have $w/(\sigma\theta)^{1/2}$ in the range 0.8 to 1.3.

Nnadi and Wilson (1992) performed experiments on 0.7 mm sand and water in a horizontal closed conduit. To make comparison, I use ε = 0.45 (the average value measured by Wang et al. 2008 for sand particle-bed collisions); α = 0.50, the tangent of the angle of repose in a channel of infinite width obtained by Forterre and Pouliquen (2003) for 0.8 mm dry sand; σ = 2.67, w = 1.63 and R = 46, from the measurements of Nnadi and Wilson (1992);

$\bar{\nu} = 0.65$, the average value of the concentration near the bed for 0.30 and 0.56 mm sand measured by Pugh and Wilson (1999). The notable fitting with the experiments shown in Fig. 4 has been obtained by setting the only parameter of the model that cannot be measured, *c*, equal to 0.65 (one experiment would actually be sufficient). The discontinuity in the derivative of the theoretical curve of Fig. 4 is due to the vanishing of the dense algebraic layer at $\breve{\theta} \approx 1.08$.

Fig. 4 also depicts the experimental results obtained by Smart (1984) and Rickenmann (1991) using gravel (diameter 4.2 to 10.5 mm) and water in flumes of inclination 4 to 11.3°. The theoretical curve of Fig. 4 has been obtained using the above mentioned parameters for sand, but for the value of the Reynolds number, that has been set equal to 2400 (valid for particles of 10 mm diameter). Fig. 4 shows that the present theory slightly underestimates the particle flow rate; this is probably due to the significant role of the downslope component of gravity in those experiments, as pointed out by Abrahams (2003). The values of the Shields parameter for the gravel experiments in Fig. 4 have not been corrected to include the role of the angle of inclination, as done instead by Smart (1984) and Rickenmann (1991); the extension of the present theory to deal with non-horizontal flows will be the subject of future works.

Conclusions

This work deals with the collisional sheet flow, i.e., the regime of sediment transport at the transition between bed and suspended load, where the particle collisions, driven by the fluid shear stress exerted at the top, dominate the momentum exchange, without being substantially affected by the turbulent fluctuations of the fluid velocity. This restricts the attention on flows characterized by a ratio of particle settling velocity to fluid shear velocity in the range one to five. Although the collisional sheet flow is somehow peculiar, its comprehension is valuable

also in view of the resemblance with more common events, such as debris flows, where the gravity plays though a key role.

In the idealized case of horizontal, steady and fully-developed flows of inelastic spheres and fluid over erodible beds, three regions have been distinguished: a diffuse collisional layer, near the top of the particles, where the set of equations provided by kinetic theory have been solved in an approximate way, using the trapezium rule of integration; a dense algebraic layer, where the algebraic balance between production and dissipation of fluctuation energy holds; and a macro-viscous layer, near the erodible bed, where the collisions are perfectly inelastic, due to the damping effect of the interstitial viscous fluid. The correlated motion between the particles that develops at high concentration (Jenkins 2006, 2007) in the dense algebraic layer has been taken into account, as well as the concentration dependence of the viscosity in the macro-viscous layer. With these and appropriate boundary conditions (no-slip and yield at the erodible bed, vanishing of the particle stresses and concentration at the top of the diffuse layer), an approximate analytical solution to the flow has been derived. The sensitivity analysis has shown that the theoretical results, in terms of particle flow rate against the Shields parameter, are strongly affected by the values of the parameter c (of order unity) in the correlation length, which is the only phenomenological parameter in the model, and cannot be therefore directly measured. However, reasonable values of c (either inferred from previous works on dry granular flows or set by fitting one experimental value of particle flow rate at a given Shields parameter) allow the theory to reproduce the experiments on the collisional sheet flows of different granular materials – plastic cylinders or sand - and water (Nnadi and Wilson 1992; Sumer et al. 1996). The role of the downslope component of gravity, for inclined flows, and the turbulent velocity fluctuations on the sediments will be included in future improvements of the present theory.

Acknowledgements

The author is grateful to Prof. James T. Jenkins for his support and discussions related to this work.

Notation

The following symbols are used in the paper:

A = coefficient;

c = parameter in the expression for the correlation length;

d = particle diameter;

D = drag force;

e = effective coefficient of restitution in wet conditions;

F = coefficient;

g = gravitational acceleration;

G = product of concentration and radial distribution function;

$\tilde{G}$ = mean value of G in the macro-viscous layer;

h = particle depth;

H = total depth of the dense algebraic and macro-viscous layers;

J = coefficient;

k = particle stress ratio at $y = H$;

L = particle correlation length;

n = coefficient of normal restitution;

p = particle pressure;

q = volume flow rate per unit width of the particles;

Q = particle energy flux;

R = particle Reynolds number;

R^* = modified Reynolds number;

s = particle shear stress;

S = fluid shear stress;

St = Stokes number;

T = granular temperature;

$\breve{T}$ = minimum granular temperature in the collisional layers;

u = particle velocity;

U = fluid velocity;

w = particle settling velocity;

x = coordinate in the flow direction;

y = coordinate in the direction perpendicular to the bed;

α = yielding value of the stress ratio at the bed;

β = coefficient of tangential restitution in a sticking collision;

δ = depth of the macro-viscous layer;

ε = effective coefficient of restitution in dry conditions;

Γ = rate of collisional dissipation;

η = fluid viscosity;

μ = coefficient;

ν = concentration;

$\bar{\nu}$ = mean concentration in the dense layers;

θ = Shields parameter;

$\breve{\theta}$ = minimum Shields parameter for having a dense algebraic layer;

$\hat{\theta}$ = maximum Shields parameter for having a macro-viscous layer;

ρ = fluid density;

σ = particle specific mass;

$\bar{\psi}$ = mean value of the generic quantity ψ in the dense algebraic layer;

ψ_a = generic quantity ψ evaluated at $y = a$.

References

Abrahams, A.D. (2003). "Bed-Load Transport Equation for Sheet Flow." *J. Hydraul. Eng.*-ASCE, 129(2), 159–163.

Armanini, A., Capart, H., Fraccarollo, L., and Larcher, M. (2005). "Rheological stratification in experimental free-surface flows of granular-liquid mixtures." *J. Fluid Mech.*, 532, 269–319.

Bagnold, R.A. (1954). "Experiments on a gravity-free dispersion of large solid spheres in a Newtonian fluid under shear." *Proc. R. Soc. Lond.* A, 225, 49–63.

Bagnold, R.A. (1973). "The Nature of Saltation and of 'Bed-Load' Transport in Water." *Proc. R. Soc. Lond.* A, 332, 473–504.

Barnocky, G., and Davis, R.H. (1988). "Elastohydrodynamic collision and rebound of spheres: Experimental verification." *Phys. Fluids*, 31, 1324.

Berzi D., and Jenkins, J.T. (2008a). "A theoretical analysis of free-surface flows of saturated granular-liquid mixtures." *J. Fluid Mech.*, 608, 393–410.

Berzi, D., and Jenkins, J.T. (2008b). "Approximate analytical solutions in a model for highly concentrated granular-fluid flows." *Phys. Rev.* E, 78, 011304.

Berzi, D., and Jenkins, J.T. (2009). "Steady inclined flows of granular-fluid mixtures." *J. Fluid Mech.*, 641, 359–387.

Berzi, D., and Jenkins, J.T. (2011). "Surface Flows of Inelastic Spheres." *Phys. Fluids*, 23, 013303.

Berzi, D., Jenkins, J.T., and Larcher, M. (2010). "Debris Flows: Recent Advances in Experiments and Modeling." *Adv. Geophys.*, 52, 103–138.

Cassar, C., Nicolas, M., and Pouliquen, O. (2005). "Submarine granular flows down inclined planes." *Phys. Fluids*, 17, 103301.

Chanson, H. (1999). *The hydraulics of open channel flow: an introduction*, Wiley, New York.

Ferguson, R.I., and Church, M. (2004). "A Simple Universal Equation for Grain Settling Velocity." *J. Sediment. Res.*, 74, 933–937.

Forterre, Y., and Pouliquen, O. (2003). "Long-surface-wave instability in dense granular flows." *J. Fluid Mech.*, 486, 21–50.

Fraccarollo, L., and Rosatti, G. (2009). "Lateral bed load experiments in a flume with strong initial transversal slope, in sub- and supercritical conditions." *Water Resour. Res.*, 45, W01419.

Garzo, V., and Dufty, J.W. (1999). "Dense fluid transport for inelastic hard spheres." *Phys. Rev.* E, 59, 5895.

Goldhirsch, I. (2003). "Rapid granular flows." *Ann. Rev. Fluid Mech.*, 35, 267–293.

Goldman, D.I., and Swinney, H.L. (2006). "Signatures of glass formation in a fluidized bed of hard spheres." *Phys. Rev. Lett.*, 96, 145702.

Herbst, O., Huthmann, M., and Zippelius, A. (2000). "Dynamics of inelastically colliding spheres with Coulomb friction: Relaxation of translational and rotational energy." *Gran. Matt.*, 2, 211–219.

Jenkins, J.T. (2006). "Dense shearing flows of inelastic disks." *Phys. Fluids*, 18, 103307.

Jenkins, J.T. (2007). "Dense inclined flows of inelastic spheres." *Gran. Matt.*, 10, 47–52.

Jenkins, J.T., and Berzi, D. (2010). "Dense Inclined Flows of Inelastic Spheres: Tests of an Extension of Kinetic Theory." *Gran. Matt.*, 12, 151–158.

Jenkins, J.T., and Hanes, D.M. (1998). "Collisional sheet flows of sediment driven by a turbulent fluid." *J. Fluid Mech.*, 370, 29–52.

Jenkins, J.T., and Savage, S.B. (1983). "A theory for the rapid flow of identical, smooth, nearly elastic particles." *J. Fluid Mech.*, 130, 187–202.

Jop, P., Forterre, Y., and Pouliquen, O. (2005). "Crucial role of sidewalls in granular surface flows: consequences for the rheology." *J. Fluid Mech.*, 451, 167–192.

Joseph, G.G., Zenit, R., Hunt, M.L., and Rosenwinkel, A.M. (2001). "Particle-wall collisions in a viscous fluid." *J. Fluid Mech.*, 433, 329–346.

Krieger, I.M., and Dougherty, T.J. (1959). "A mechanism for non-Newtonian flow in suspensions of rigid spheres." *J. Rheol.*, 3, 137–152.

Lorenz, A., Tuozzolo, C., and Louge, M.Y. (1997). “Measurements of impact properties of small, nearly spherical particles." *Exp. Mech.*, 37, 292–298.

Mitarai, N., and Nakanishi, H. (2007). “Velocity correlations in dense granular shear flows: Effects on energy dissipation and normal stress.” *Phys. Rev.* E, 75, 031305.

Nnadi, F.N., and Wilson, K.C. (1992). “Motion of Contact-Load Particles at High Shear Stress.”, *J. Hydraul. Eng.*-ASCE, 118(12), 1670–1684.

Olafsen, J.S., and Urbach, J.S. (1998). “ Clustering, Order , and Collapse in a driven granular monolayer.” *Phys. Rev. Lett.*, 81, 4369–4372.

Ovarlez, G., Bertrand, F., and Rodts, S. (2006). “Local determination of the constitutive law of a dense suspension of noncolloidal particles through magnetic resonance imaging.” *J. Rheol.*, 50, 259–292.

Pasini, J.M., and Jenkins, J.T. (2005). “Aeolian transport with collisional suspension.” *Phil. Trans. R. Soc.* A, 363, 1625–1646.

Pugh, F.J., and Wilson, K.C. (1999). “Velocity and Concentration Distributions in Sheet Flow above Plane Beds.” *J. Hydraul. Eng.*-ASCE, 125(2), 117–125.

Rickenmann, D. (1991). “Hyperconcentrated Flow and Sediment Transport at Steep Slopes.” *J. Hydraul. Eng.*-ASCE, 117(11), 1419–1439.

Savage, S.B. (1984). “The mechanics of rapid granular flows.” *Adv. Appl. Mech.*, 24, 289–366.

Smart, G.M. (1984). “Sediment Transport Formula for Steep Channels.” *J. Hydraul. Eng.*-ASCE, 110(3), 267–276.

Sumer, B.M., Kozakiewicz, A., Fredsoe, J., and Deigaard, R. (1996). “Velocity and concentration profiles in sheet-flow layer of movable bed.” *J. Hydraul. Eng.*-ASCE, 122(10), 549–558.

Torquato, S. (1995). “Nearest-neighbor statistics for packings of hard spheres and disks.” *Phys. Rev.* E, 51, 3170–3182.

Wang, D., Wang, Y., Yang, B., and Zhang, W. (2008). “Statistical analysis of sand grain/bed collision process recorded by high-speed digital camera.” *Sedimentology*, 55(2), 461–470.

Wilson, K.C. (1987). “Analysis of bed-load motion at high shear stress.” *J. Hydraul. Eng.*-ASCE, 113(1), 97–103.

List of tables

Table 1. Summary of the adopted constitutive relations in the collisional layers.

$p = 4\nu GFT$
$F = (1+e)/2 + 1/(4G)$
$\frac{1-\varepsilon^2}{4} \equiv \frac{1-n^2}{4} + \frac{1+\beta}{7} - \left(\frac{1+\beta}{7}\right)^2 \left[1 + \frac{5(1+\beta)}{14-5(1+\beta)}\right]$
$s = \mu u'$
$\mu = \left(2J/5\pi^{1/2}\right) p/\left(FT^{1/2}\right)$
$J = \frac{(1+e)}{2} + \frac{\pi}{32} \frac{\left[5+2(1+e)(3e-1)G\right]\left[5+4(1+e)G\right]}{\left[24-6(1-e)^2-5(1-e^2)\right]G^2}$
$\Gamma = 12\nu G(1-e^2)T^{3/2}/\left(\pi^{1/2}L\right)$
$L = \max\left[1, \left(0.5cG^{1/3}u'/T^{1/2}\right)\right]$

Figure1
Click here to download high resolution image

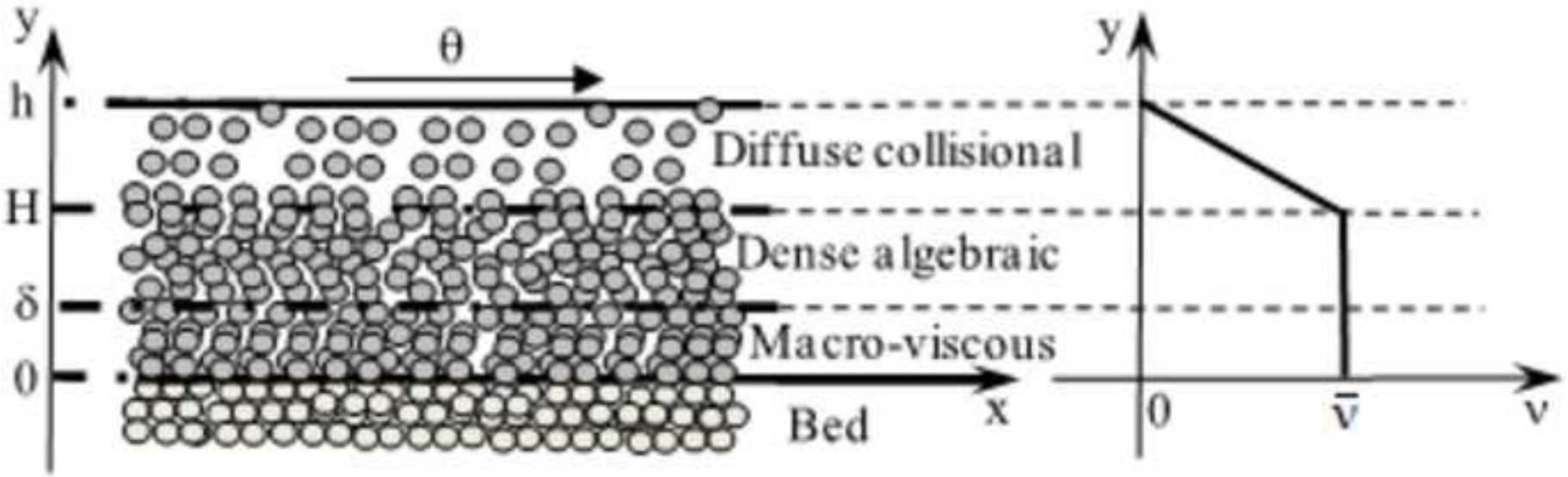

Figure2

Click here to download high resolution image

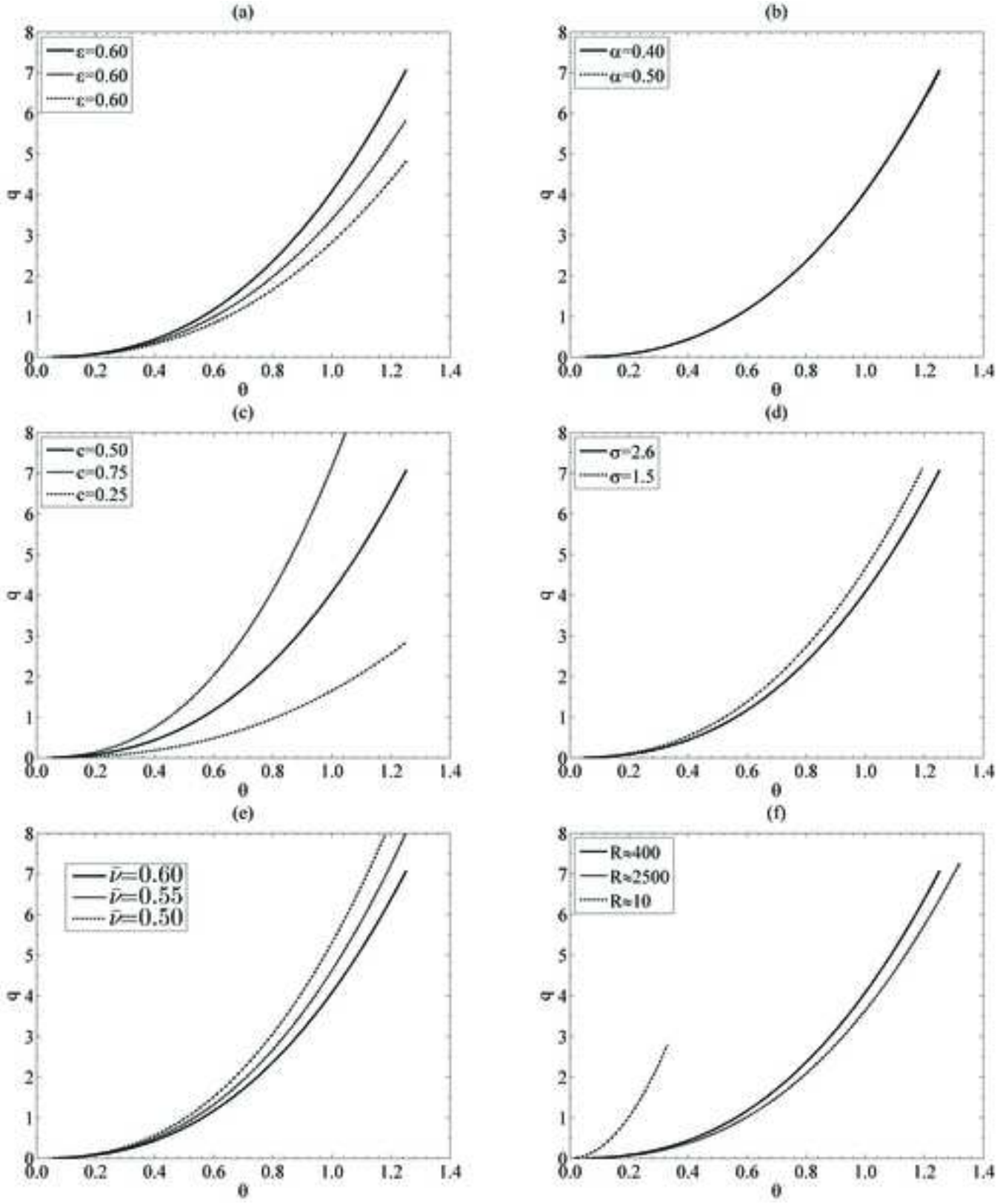

Figure3
Click here to download high resolution image

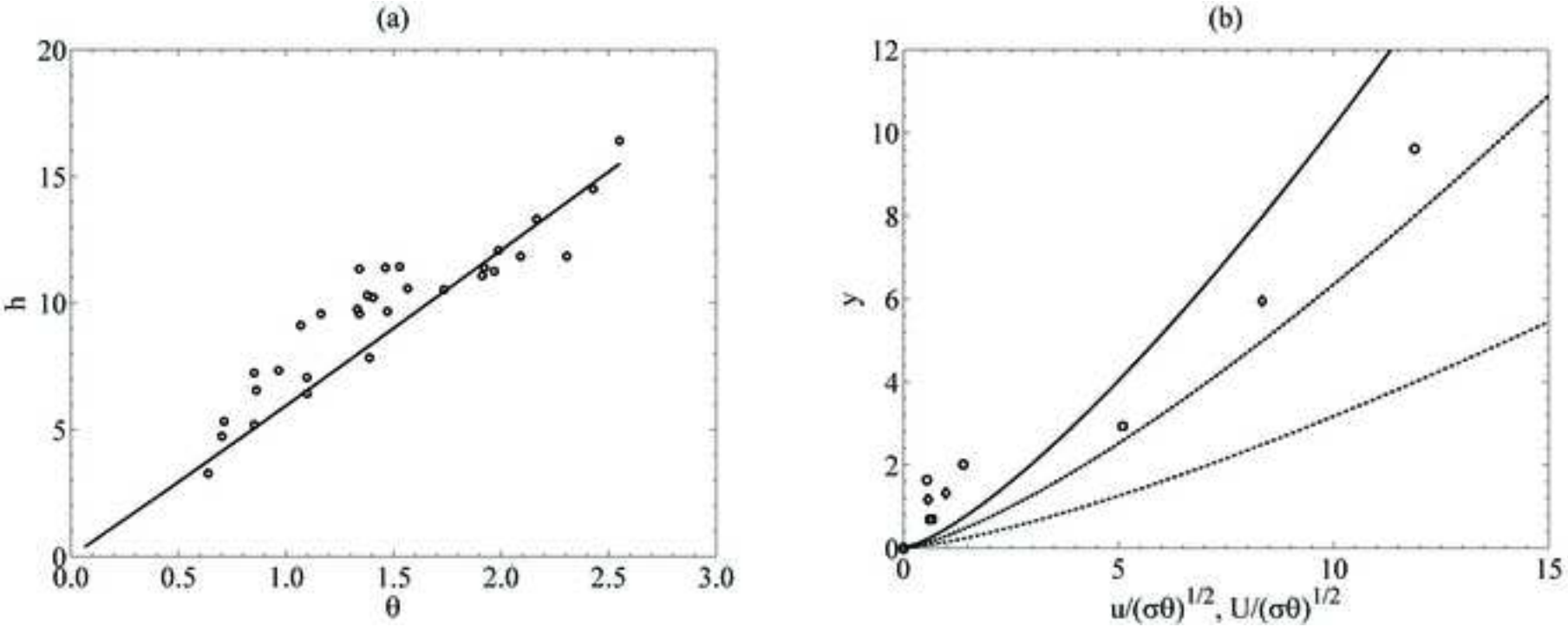

Figure4

Click here to download high resolution image

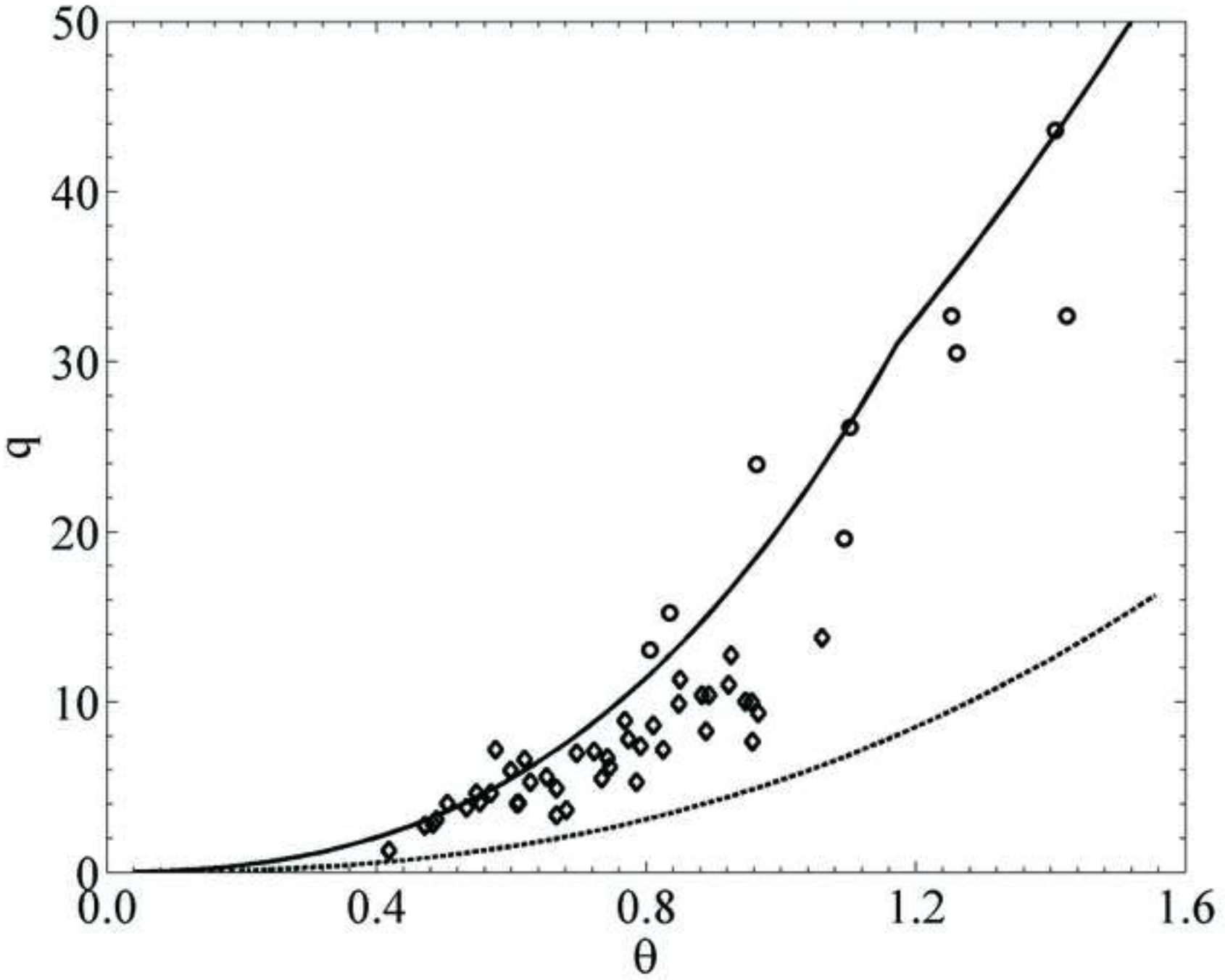

List of figure captions

Figure 1. Sketch of the flow configuration with the frame of reference and the assumed concentration profile.

Figure 2. Sensitivity of the volume flow rate per unit width of the particles as a function of the Shields parameter to: (a) the restitution coefficient in dry condition; (b) the yielding stress ratio; (c) the parameter *c* in the correlation length; (d) the particle specific mass; (e) the approximately constant concentration in the dense layers; (f) the Reynolds number of the particles. In all the plots, the solid line represents the reference solution (see the text for more details).

Figure 3. (a) Experimental (circles) and theoretical (lines) particle depth versus the Shields parameter. (b) Particle (symbols, present theory) and fluid (lines, from Eq. 3-26) scaled velocity versus the distance from the bed for: $\theta = 0.50$ (dot-dashed line and squares); $\theta = 1.00$ (dashed line and diamonds); $\theta = 1.60$ (solid line and circles). The plots refer to the flow of 3 mm plastic cylinders and water.

Figure 4. Experimental (symbols) and theoretical (lines) volume flow rate per unit width of the particles versus the Shields parameter for sand (circles and solid line) and gravel (diamonds and dashed line).